Partial-wave analysis of multiphoton ionization of sodium by short laser pulses in over-the-barrier regime

A. Bunjac, D. B. Popović, N. S. Simonović

Institute of Physics Belgrade, Serbia

2020

Introduction

Freeman et al. (PRL **59**, 1092 (1987)) have shown that when an atomic state during the laser pulse transiently shifts into resonance due to the dynamic (AC) Stark shift, the resonantly-enhanced-multiphoton-ionization (REMPI) takes place, increasing the photoelectron yield, and one observes a peak at the corresponding value of photo-electron energy – *Freeman resonance*.

A particular challenge is *the selective ionization* of the atom through a single energy level which could produce a high ion yield. By increasing the laser intensity one increases the yield, but also spreads the electron population over multiple energy levels and, in turn, reduces the selectivity. Hart et al. (PRA **93**, 063426 (2016)) have shown that such a process could be achieved by controlling the resonant dynamic Stark shift of sodium states via intensity of the laser pulse of an appropriate wavelength.

Here we study the multiphoton ionization (MPI) of the sodium atom by the laser pulse of 800 nm wavelength and 57 fs full width at half maximum (FWHM) with the peak intensities ranging from 3.5 to 8.8 $\mathrm{TW/cm^2}$, which are the same values as used in the experiment by Hart et al.

The Model

Within the single-electron model the dynamics of the valence (active) electron of sodium atom in an alternating electric field $F(t)$ is described by Hamiltonian (in atomic units)

$$H = \frac{\vec{p}^2}{2} + V_{\text{core}}(r) - F(t)z.$$

The effective core potential $V_{\text{core}}(r)$ describes the interaction of the valence electron with the atomic core. For this purpose we use the Hellmann's pseudopotential

$$V_{\text{core}}(r) = -\frac{1}{r} + \frac{A}{r}\, e^{-ar}.$$

The parameters $A = 21$ and $a = 2.54920$ provide the correct value for the ionization potential of sodium $I_{\text{p}} = 5.1391\,\text{eV} = 0.18886\,\text{a.u.}$ and reproduce approximately the energies of singly-excited states (see Fig. 1).

We consider a linearly polarized laser pulse of the form

$$F(t) = F_{\text{peak}} \sin^2(\pi t/T_{\text{p}}) \cos(\omega t), \quad 0 < t < T_{\text{p}}$$

(otherwise $F(t) = 0$). Due to the axial symmetry of the system, the magnetic quantum number m of the valence electron is a good quantum number and we set the ground state value $m = 0$.

Energy Scheme and Photoionization Channels

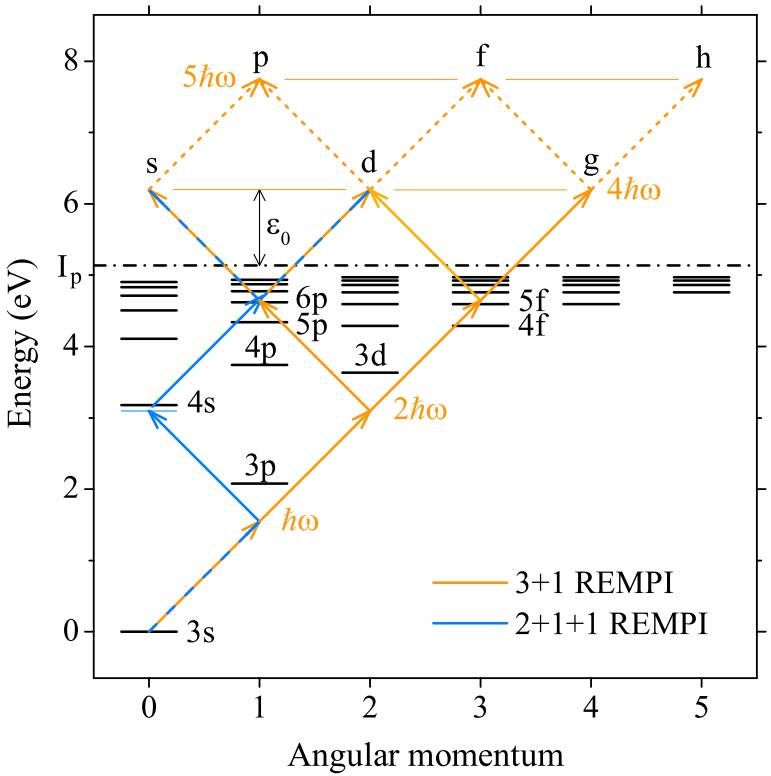

Figure 1. The unperturbed energy levels (short black lines) corresponding to singly excited states of sodium relative to its ground state (3s) and possible 4-photon and 5-photon absorption pathways (arrows) from the ground state to continuum for the radiation of 800 nm wavelength ($\hbar\omega \approx 1.55$ eV). The continuum boundary is drown by the dash-dot line and ϵ_0 is the excess energy of photoelectrons produced in the nonresonat 4-photon ionization.

At 800 nm wavelenghth there are three dominant REMPI channels:
(i) (3+1)-photon ionization via excitation of 5p, 6p and 7p states, giving rise to photoelectrons with s and d-symmetry;
(ii) (3+1)-photon ionization via excitation of 4f, 5f and 6f states, producing photoelectrons with d and g-symmetry;
(iii) (2+1+1)-photon ionization via nearly resonant two-photon transition 3s $\rightarrow$ 4s and subsequent excitation of P-states, giving rise to photoelectrons with s and d-symmetry.

Photoelectron momentum distribution

The photoionization process is simulated by calculating the evolution of the wave function of valence electron $\psi(\vec{r}, t)$, which is initially (at $t = 0$) chosen to be the lowest eigenstate of Hamiltonian H (for $F = 0$) that describes the sodium ground state. The evolution is calculated by integrating the time-dependent-Schrödinger-equation (see Bunjac et al., PCCP **19**, 19829 (2017)).

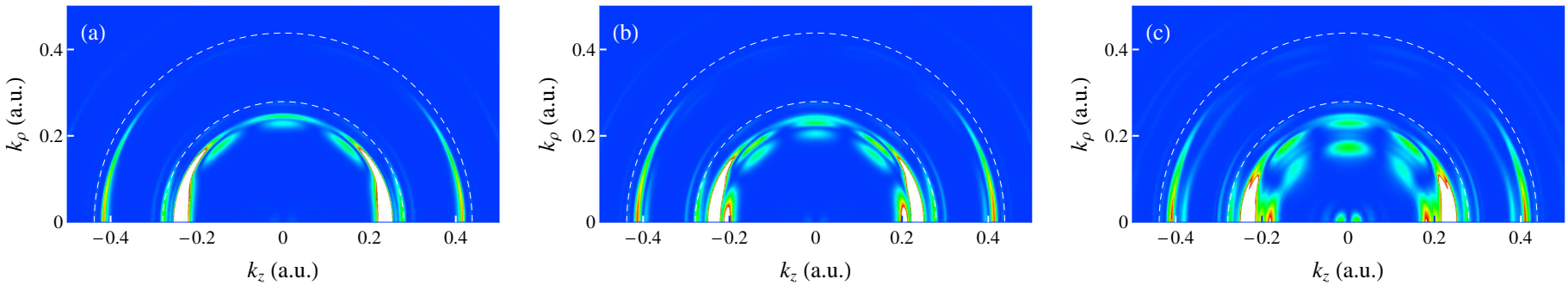

Figure 2. Photoelectron momentum distribution $|\bar{\psi}(\vec{k})|^2$ in the photoionization of sodium by the laser pulse ($\lambda = 800\,\text{nm}$, $T_p = 2 \times \text{FWHM} = 114\,\text{fs}$) calculated at $t = 145\,\text{fs}$ for three values of the laser peak intensity: (a) $3.5\,\text{TW/cm}^2$, (b) $4.9\,\text{TW/cm}^2$ and (c) $8.8\,\text{TW/cm}^2$. The dashed semicircles of radii $k_0 = 0.279\,\text{a.u.}$ and $k_0' = 0.438\,\text{a.u.}$ correspond to the asymptotic values of the photoelectron momentum in the weak field limit after absorption of four and five photons (the threshold and the 1st ATI order), respectively.

Partial wave analysis

In order to determine and analyze the photoelectron energy spectrum (PES), the outgoing part of the active electron wave function $\psi(\vec{r}, t)$ at a time $t > T_p$ is transformed from the coordinate to momentum representation $\bar{\psi}(\vec{k}, t)$ by the Fourier transform and expanded in terms of partial waves

$$\bar{\psi}(\vec{k}) = \sum_{\ell} \Phi_\ell(k)\, Y_{\ell 0}(\vartheta),$$

where $Y_{\ell 0}(\vartheta)$ are the spherical harmonics with $m = 0$ and $\Phi_\ell(k) = \int Y^*_{\ell 0}(\vartheta)\, \bar{\psi}(\vec{k})\, \mathrm{d}\Omega$ are the corresponding radial functions. Using the representation of $\bar{\psi}$ in cylindrical coordinates, the radial functions can be calculated as

$$\Phi_\ell(k) = 2\pi \int_0^\pi \bar{\psi}(k \sin\vartheta, k\cos\vartheta)\; Y_{\ell 0}(\vartheta)\; \sin\vartheta\, \mathrm{d}\vartheta.$$

The radial probability density of photoelectrons in momentum space is the sum $w(k) = \sum_\ell w_\ell(k)$, where

$$w_\ell(k) = |\Phi_\ell(k)|^2\, k^2$$

are the partial probability densities. The radial probability density w as a function of the photoelectron energy $\epsilon = \hbar^2 k^2/(2m_e)$ represents PES.

Partial probability densities and PES

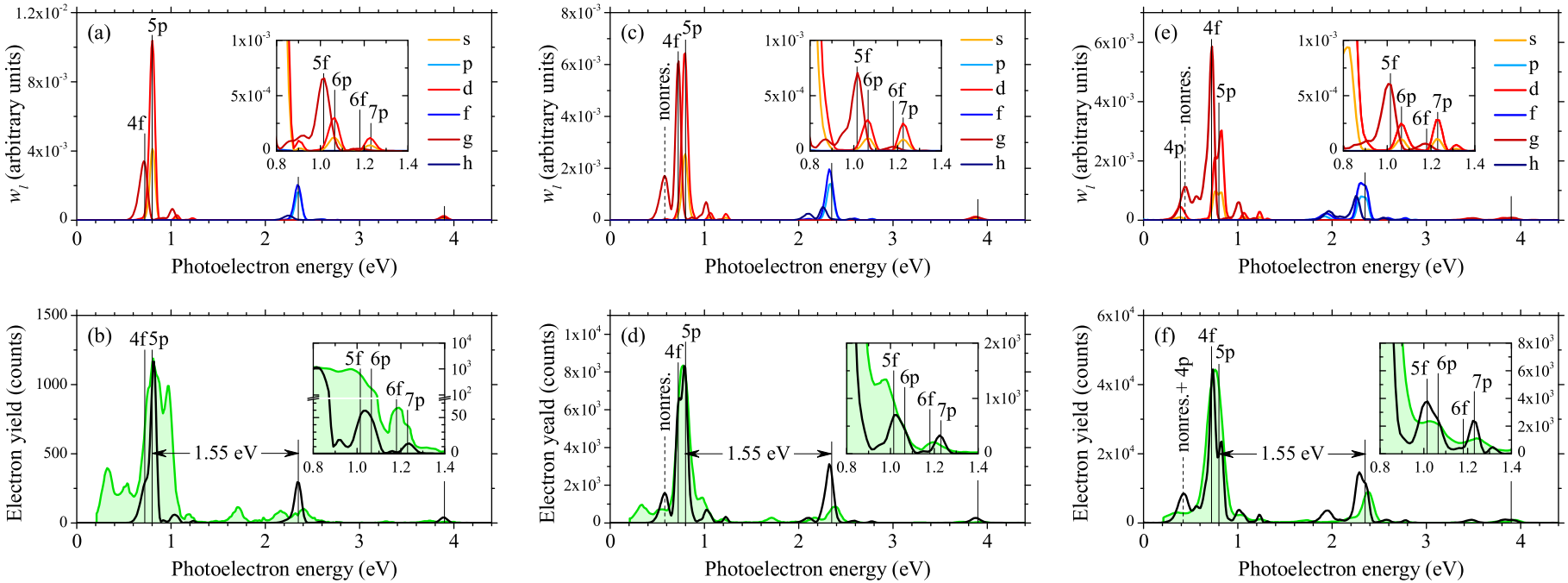

Figure 3. Partial probability densities w_ℓ for $\ell = 0, \ldots, 5$ (top, lines of different color) and the total probability density w (bottom, black line) as functions of the photoelectron energy $\epsilon = \hbar^2 k^2/(2m_e)$ obtained at three values of the laser peak intensity: (a,b) 3.5 TW/cm^2, (c,d) 4.9 TW/cm^2, (e,f) 8.8 TW/cm^2. Experimental PES (Hart et al., 2016) are represented by full green lines (bottom). The full vertical lines mark the energies of two REMPI channels (via f and p states) of the threshold peak as well as the position of 5p subpeak in the higher order ATI peaks.

Conclusions

The spectra, both the calculated and experimental, exhibit a typical *above threshold ionization (ATI)* structure with prominent peaks separated by the photon energy $\hbar\omega \approx 1.55\,\mathrm{eV}$. Fig. 3 shows the peaks corresponding to lowest three orders of ATI (MPI by $4+s$ photons, $s=0,1,2$) which are located approximately at $\epsilon = 0.8\,\mathrm{eV} + s\hbar\omega$.

The partial wave analysis recovers the character of ATI peaks. We see in Fig. 3 (top) that for the photoelectron energies around the main peak ($s=0$, $\epsilon \approx 0.8\,\mathrm{eV}$) and around the second-order ATI peak ($s=2$, $\epsilon \approx 3.9\,\mathrm{eV}$) dominant contributions in the total probability density come from the partial waves with even ℓ (s, d, g-waves). Thus, the photoelectrons with these energies are generated by absorbing an *even* number of photons ($N=4$ and 6). Contrarily, in the vicinity of the first-order ATI peak ($s=1$, $\epsilon \approx 2.35\,\mathrm{eV}$) the partial waves with even ℓ are suppressed and those with odd ℓ (p, f, h-waves) dominate. Therefore, in this case *odd* number of photons is absorbed (here $N=5$).

Fig. 3 (top) shows that at the laser peak intensity of $3.5\,\mathrm{TW/cm^2}$ dominant contribution in the main peak (around 0.8 eV) comes from d-electrons, while at the intensity of $8.8\mathrm{TW/cm^2}$ the electrons of g-symmetry dominate. Therefore, *by changing the laser intensity, one selects the main ionization channel* – in the first case this is the 3+1 (or 2+1+1) REMPI via 5p state, while in the second case it is the 3+1 REMPI via 4f state.